

Photoluminescence study of the 1.047 eV emission in GaN

K. Pressel^{a)} and S. Nilsson

Institut für Halbleiterphysik, P.O. Box 409, 15204 Frankfurt/Oder, Germany

R. Heitz and A. Hoffmann

Techn. Univ. Berlin, Hardensbergstr. 36, 10623 Berlin, Germany

B. K. Meyer

Physik-Department E16, Techn. Univ. München, 85748 Garching, Germany

(Received 20 June 1995; accepted for publication 1 December 1995)

We use photoluminescence to study residual transition metal contaminants in GaN layers, which are grown by the sandwich technique either on 6H-SiC substrate or on sapphire substrate. We observe three no-phonon lines in the near infrared optical region at 1.3 eV, 1.19 eV, and 1.047 eV caused by 3d transition metals. The appearance of GaN related host modes in the phonon sideband of these emissions proves that the luminescence centers are incorporated in the hexagonal GaN layers. In this paper we especially focus on the luminescence band with the no-phonon line at 1.047 eV. Temperature dependent photoluminescence measurements reveal an excited state splitting of 8 meV. In photoluminescence excitation spectroscopy we observe a further excited state at 1.6 eV with a fine structure splitting. The appearance of this excited state in the n-type samples gives evidence that the defect must already exist in its luminescent charge state without illumination. The experimental results on the 1.047 eV emission fit to a $4T_2(F) \rightarrow 4A_2(F)$ internal electronic transition of a transition metal with a $3d^7$ electronic configuration. © 1996 American Institute of Physics.
[S0021-8979(96)08905-4]

I. INTRODUCTION

In the last few years the interest in GaN epitaxial layers has been strongly increased, because the problem of p-doping was solved.¹ Thus, the realization of an InGaN/AlGaIn blue green light emitting diode, which has a much higher quantum efficiency than the SiC blue light emitting diode, became possible.² Presently the wide bandgap semiconductor GaN is intensively studied to develop a blue laser diode.³

The knowledge of the behavior of deep defects is very important to be able to optimize electrical and optical devices. Especially 3d elements act as deep defects and appear as natural contaminants during crystal growth. The 3d elements show sharp and characteristic line patterns in photoluminescence (PL) experiments which are due to internal transitions in the 3d-shell. Up to now only a few optical studies have been performed on transition metals in GaN.⁴⁻⁶ In these studies the GaN layers were grown on sapphire substrate either by metal organic vapor phase epitaxy (MOVPE) or vapor phase epitaxy (VPE).

In this article we used photoluminescence to search for transition metals which are introduced as natural contaminants in GaN grown by the sandwich technique. The GaN samples show three characteristic luminescence bands with no-phonon (NP) lines peaking at 1.3 eV, 1.19 eV, and 1.047 eV which are caused by residual transition metal ions incorporated during crystal growth. Especially the 1.19 eV is very intense. Thus one can think of developing a light emitting diode in the near infrared optical region similar to the Er^{3+} internal 4f emission in GaAs⁷ and Yb^{3+} emission in InP.⁸ The 1.3 eV emission and the 1.19 eV emission have already

been observed in GaN samples grown by MOVPE and VPE.⁴⁻⁶ In this article we mainly focus on the new emission at 1.047 eV, which has not been observed as natural contaminant in GaN samples grown by MOVPE and VPE.

II. EXPERIMENT

A major problem of the growth of GaN, which mainly crystallizes in the wurtzite structure, is the lack of a proper substrate material. Usually sapphire is used which has a lattice mismatch of ~16% to GaN. Our GaN samples were not only grown on sapphire but also on 6H-SiC or freestanding directly on graphite by a modification of the sublimation sandwich technique.^{9,10} Compared to the sapphire substrate, which is mainly used by crystal growers, the 6H-SiC substrate reduces the lattice mismatch to 3.5%. The layers are usually n-type conductive with free carrier concentrations between 2×10^{17} and $1 \times 10^{18} \text{ cm}^{-3}$. The thickness of the layers is more than 10 μm . More details on the promising quality of the GaN/6H-SiC samples are published elsewhere.^{11,12}

The samples were excited with an Ar ion laser (514 nm or UV) or in some cases with a Kr ion laser (647 nm). The PL measurements were performed using a BOMEM DA8.02 Fourier-transform infrared spectrometer. The PL excitation (PLE) measurements were performed with conventional monochromator technique and a quartz halogen lamp. For all the measurements a cooled Ge-detector was used.

We tried doping of GaN with transition metals during crystal growth, by diffusion, and also by ion implantation. All these efforts were not successful and more careful studies to optimize intentional doping with transition metals have to be performed:

^{a)}Electronic mail: pressel@ihp.d400-gw.de

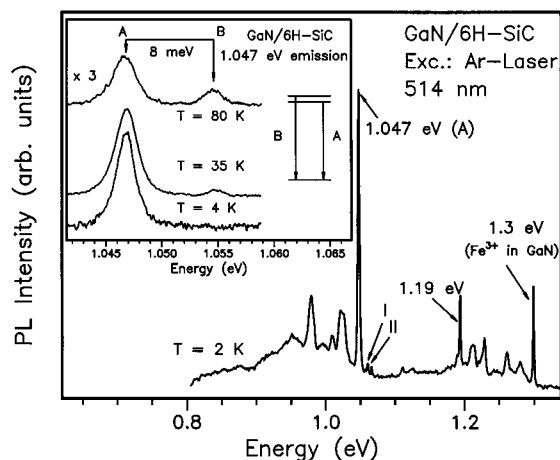


FIG. 1. Photoluminescence (PL) spectra of GaN/6H-SiC in the region between 0.8 and 1.35 eV. Three no-phonon lines peaking at 1.3 eV, 1.19 eV, and 1.047 eV (A) appear by Ar ion laser (514 nm) excitation. The inset shows three spectra detected at 4 K, 35 K, and 80 K. With rising temperature to the no-phonon line at 1.047 eV, labelled A, the hot line, labelled B, appears. The corresponding level scheme is shown in the right part.

- Preliminary experiments of intentional doping of GaN during crystal growth by the sandwich technique resulted in GaN samples of unsatisfied quality.
- In first diffusion experiments (between 700 °C and 900 °C) it was not possible to introduce transition metals. One problem is the evaporation of nitrogen at such high temperatures.
- The appearance of emissions in ion implanted samples did strongly depend on the annealing conditions.

All the various complexes that are generated are presently difficult to attribute and beyond the scope of this paper. A clear identification of the transition metals from the implantation data is not possible. Therefore a careful characterization of the luminescence centers, which are caused by unintentional doping with transition metals during crystal growth, is very important.

III. EXPERIMENTAL RESULTS

Figure 1 shows a typical near-infrared spectrum of a GaN sample grown on 6H-SiC by the sandwich technique. The sample is excited with the below bandgap green line (514 nm) of the Ar ion laser. Three strong and characteristic NP lines peaking at 1.3 eV, 1.19 eV, and 1.047 eV as well as the corresponding richly structured phonon sidebands are observed. All the three emissions can also be excited by above bandgap excitation with UV light of the Ar ion laser. They also appear in the GaN samples grown on sapphire substrate or freestanding directly on graphite by the sandwich technique. While the luminescence bands at 1.3 eV and 1.19 eV are also detected in GaN samples grown on sapphire by MOVPE and VPE, we only observe the 1.047 eV emission in samples grown by the sandwich technique.

Due to their sharpness and their energy positions in the near infrared region the three NP lines are attributed to internal electronic transitions of different 3d elements. In temperature dependent measurements up to 100 K we only observe a small red shift of the NP lines of less than 1 meV

which is typical for an internal electronic transition of a 3d element. When scanning the laser spot across the sample the change of the energetic positions of the defects is less than 0.1 meV. The linewidths change up to 10 % on the samples, which is caused by different local strain. While the lineshape of the 1.3 eV emission is asymmetric the lineshape of the 1.19 eV and 1.047 eV emission are symmetric and Lorentzian at 2 K. Polarization measurements were not successful. Because of the small size of the sample (usually 2 mm²) and the thin layers we observed a too weak signal when the sample is excited perpendicular to the direction of the surface.

The luminescence band with the NP line at 1.3 eV was first reported by Maier *et al.*⁴ in GaN samples grown on sapphire substrate. Based on temperature dependent PL measurements, ESR-, ODMR studies,^{4,5} and Zeeman measurements up to 15 Tesla¹³ it was attributed to an internal 3d transition of Fe³⁺ (⁴T₁ → ⁶A₁). Fe seems to be a predominant contaminant that can easily be introduced into GaN during crystal growth. In most of our investigated MOVPE-samples, VPE-samples, and in the samples grown by the modified sandwich technique we could resolve at least weak traces of the 1.3 eV emission.

The emission at 1.19 eV was first reported by Baur *et al.*⁵ They tentatively assigned it to an internal 3d transition of Cr⁴⁺. According to our experimental results this emission is caused by the ¹E(D) → ³A₂(F) internal electronic transition of Ti²⁺. A detailed study of the 1.19 eV luminescence band will be published elsewhere.¹⁴

In the following we mainly focus on the emission at 1.047 eV. We did not observe this emission in GaN samples grown by MOVPE or VPE. One reason might be that the growth temperature used for the sandwich technique is about 1100 °C compared to the 1000 °C used for MOVPE and VPE.

The emissions labelled I and II in Fig. 1 do not originate from this defect because in contrast to the 1.047 eV emission they were not observed in spectra excited with the 647 nm red light of a Kr ion laser. The inset of Fig. 1 shows three detailed PL spectra in the optical range of the NP line at 1.047 eV (labelled A) detected at different temperatures. With rising temperature a hot line (labelled B) shows up 8 meV higher in energy, which indicates a splitting of the excited state. The corresponding level scheme is depicted in the inset of Fig. 1.

Figure 2 shows the phonon sideband of the 1.047 eV emission in comparison to the phonon sidebands of the 1.3 eV emission (Fe³⁺) and the 1.19 eV emission (Ti²⁺). Additionally the phonon sideband of Fe³⁺ in ZnO is depicted to show the close correlation between the two wurtzite semiconductor materials GaN and ZnO. It is easier to compare the phonon sidebands if all the NP lines are on the same positions. Thus, we transferred the positions of all the NP lines to the energy of the 1.047 eV emission. The top scale indicates the energetic distance of the phonon replica to the NP lines. In the lower part of Fig. 2 the positions of the phonon modes of GaN observed in Raman spectroscopy¹⁵ are indicated by arrows.

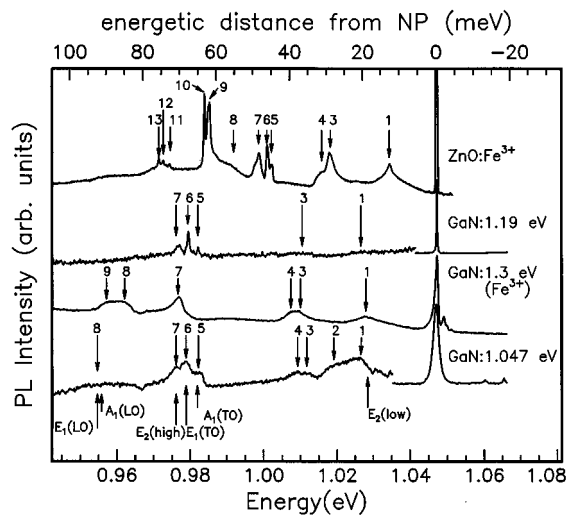


FIG. 2. Comparison of the phonon sideband of the 1.047 eV emission with the phonon sideband of Fe^{3+} in GaN, the phonon sideband of the 1.19 eV emission, and the phonon sideband of Fe^{3+} in ZnO. The top scale indicates the distance of the phonon replica from the no-phonon lines. Below the positions of the phonon modes observed from Raman spectroscopy are indicated (compare Table I). The emissions are normalized to the 1.047 eV line in GaN. In the sidebands structures are observed that coincide with modes observed in Raman spectroscopy.

In Table I the characteristic phonon modes observed for GaN¹⁵ (column 1) and ZnO¹⁶ (column 5) in Raman spectroscopy are summarized. Furthermore the phonon energies in the sidebands, determined from Fig. 2, of the 1.047 eV (column 2), of the 1.19 eV (column 3), of the 1.3 eV (column 4) emissions in GaN, and of the Fe^{3+} emission in ZnO¹⁷ (column 6) are given.

TABLE I. Energies of the phonon replica (determined from Fig. 2) of the three defect emissions with no-phonon lines at 1.047 eV (column 2), 1.19 eV (column 3), 1.3 eV (column 4), and Fe^{3+} in ZnO (column 6). The energies of the phonon modes is first given in cm^{-1} (for better comparison with Raman data) and then in meV. The numbers in brackets belong to the maxima according to Fig. 2. Phonon modes of hexagonal GaN [average values according to Kozawa *et al.* (Ref. 15)] and [ZnO (Ref. 16)], determined from Raman spectroscopy, are summarized in the first and fifth column, respectively.

Raman modes GaN	1.047 eV	1.19 eV	1.3 eV	Raman modes ZnO	Fe^{3+} in ZnO
(Kozawa <i>et al.</i> ^a)			(Fe^{3+} in GaN)	(LB ^b)	(Heitz <i>et al.</i> ^c)
$\text{cm}^{-1}/\text{meV}$	$\text{cm}^{-1}/\text{meV}$	$\text{cm}^{-1}/\text{meV}$	$\text{cm}^{-1}/\text{meV}$	$\text{cm}^{-1}/\text{meV}$	$\text{cm}^{-1}/\text{meV}$
$E_2(\text{low})$: 144/17.9	169/21.0 (1) 219.4/27.2 (2) 286.8/35.6 (3) 308.4/38.2 (4)	~170/21.1 (1) ~295/36.6 (3)	154/19.1 (1) 301/37.3 (3) 316/39.2 (4)	$E_2(\text{low})$: 101/12.5	102.7/12.7 (1) 241.2/29.9 (3) 271.2/33.6 (4)
$E_2(\text{high})$: 570/70.7	569.4/70.6 (7)	569.0/70.5 (7)	569.3/70.6 (7)	$E_2(\text{high})$: 437/54.2	457/56.7 (8)
$A_1(\text{TO})$: 532/66	527.8/65.4 (5)	524.8/65.1 (5)		$A_1(\text{TO})$: 380/47.1	372.2/46.1 (5) 387/48.0 (6)
$E_1(\text{TO})$: 561/69.6	549.9/68.2 (6)	547/67.8 (6)		$E_1(\text{TO})$: 407/50.5	399.2/49.5 (7) 510/63.2 (9) 522/64.7 (10)
$A_1(\text{LO})$: 736/91.2	~		690/85.6 (8)	$A_1(\text{LO})$: 574/71.2	601.3/74.5 (11)
$E_1(\text{LO})$: 745/92.4	750/93.0 (8)		717/88.9 (9)	$E_1(\text{LO})$: 583/72.3	610/75.6 (12) 625.2/77.5 (13)

^aReference 15.

^bReference 16.

^cReference 17.

The phonon sidebands (Fig. 2) of the three 3d elements in GaN show structures separated by approximately 19 meV (labelled 1 in all the sidebands) from the NP lines. These structures are close to the $E_2(\text{low})$ observed in Raman spectroscopy. The spectrum on top shows the phonon sideband of the Fe^{3+} (${}^4T_1 \rightarrow {}^6A_1$) transition in the II/VI semiconductor ZnO,¹⁷ which has similar properties as GaN. In the phonon sideband of Fe^{3+} in ZnO we also observe a structure, labelled 1, close to the $E_2(\text{low})$.

To the modes at about 40 meV (3,4) in the sideband of the 1.047 eV emission no Raman related phonon modes are known. Structures labelled 3 and 4 also appear in the sideband of Fe^{3+} in ZnO. We attribute both the structures 3 and 4 in the 1.047 eV sideband of GaN and the structures 3 and 4 in the sideband of Fe^{3+} in ZnO to acoustical phonons. Because of the similarities of GaN and ZnO these structures seem to have the same origin. A detailed interpretation is not possible up to now because no complete phonon dispersion of GaN is available.

In the sideband of the 1.19 eV emission and the 1.047 eV emission three modes, labelled 5 to 7, appear that almost coincide with the $A_1(\text{TO})$, $E_1(\text{TO})$, and $E_2(\text{high})$ (Table I) of GaN. The Fe^{3+} sideband in GaN shows only the structure 7 that is close to $E_2(\text{high})$. For Fe^{3+} in ZnO there also appear modes that are close to the $A_1(\text{TO})(5)$, $E_1(\text{TO})(7)$, and $E_2(\text{high})(8)$ Raman modes.

The characteristic maxima in the sidebands, which are close to modes observed in the Raman spectrum¹⁵ of hexagonal GaN, indicate that all the three emissions with NP lines at 1.047 eV, 1.19 eV, and 1.3 eV are caused by transition metal atoms on substitutional site in the wurtzite GaN host. The appearance of the GaN related phonon replica exclude that

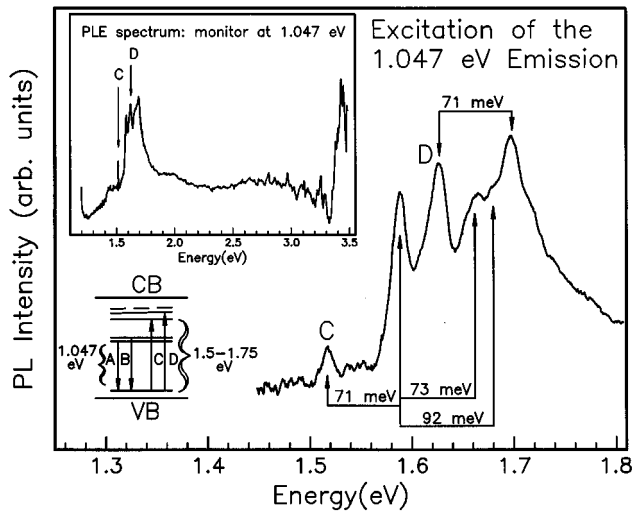


FIG. 3. Photoluminescence (PL) excitation spectrum of the 1.047 eV emission. The monitor wavelength was set to 1.047 eV. On a broad background we observe not only excitation in the near bandedge region (about 3.4 eV) but also strong below bandgap peaks in the range between 1.5 eV and 1.75 eV. We observe at least two no-phonon transitions labelled C and D. GaN related phonon modes couple to these transitions (see Table 1 and Fig. 2). The PL excitation data reveal that the luminescence center is already present in the dark. The suggested level scheme of this defect in the bandgap is indicated in the inset (for the transitions A and B: see Fig. 1).

the emissions are caused by luminescence centers in the substrate.

The inset of Fig. 3 shows a PLE spectrum of the 1.047 eV emission. We clearly see that this emission can be excited with light not only in the near bandedge region at energies higher than 3.35 eV but also in the optical range between 1.5 eV and 1.75 eV. All the features are superimposed on a broad background signal.

The spectrum of Fig. 3 shows the very strong enhancement of the PL intensity in the range between 1.45 eV and 1.8 eV in detail. A set of at least six peaks can be observed. The peaks labelled C (1.518 eV) and D (1.618 eV) belong to NP lines. The other four peaks can be explained by coupling to phonon modes, which are summarized in Table I (compare Fig. 2). A phonon with energy 71 meV (due to $E_2(\text{high})$) couples to the absorptions C and D. The two peaks at 1.662 and 1.681 eV can be attributed to a two-phonon coupling to the absorption C: 71 meV ($E_2(\text{high})$)+73 meV ($\sim E_2(\text{high})$) and 71 meV ($E_2(\text{high})$)+92 meV ($A_1(\text{LO})$, $E_1(\text{LO})$).

The peaks are relatively sharp and therefore a charge-transfer transition can be most definitely excluded. The PLE measurements reveal a higher excited state of the luminescence center by which the 1.047 eV emission can be excited. The two NP lines C and D belong to a fine structure splitting of this excited state. The deduced level scheme of the defect with the two transitions A and B, observed in PL, and the two absorptions C and D, observed in PLE, is depicted in the left part of Fig. 3. We assume that the higher excited state observed in PLE is still in the bandgap because otherwise the fine structure lines should be broader. From the PLE spectra it can be concluded that the defect is already in its lumines-

cent charge state in the dark (without laser excitation) in the n-type material.

IV. DISCUSSION

In analogy to other III/V and II/VI semiconductors and in agreement with the appearance of phonon modes of hexagonal GaN in the phonon sidebands, the 3d elements are incorporated on the Ga lattice site. Therefore 3d elements are tetrahedrally surrounded by four nitrogen next nearest neighbors. The main splitting of the 3d levels is caused by the tetrahedral crystal field. Further spin-orbit coupling leads to an additional splitting. The wurtzite structure mostly causes a weak deviation from the pure tetrahedral case leading to C_{3v} symmetry. This reduction to C_{3v} symmetry causes a weak additional splitting which is in the range of only a few cm^{-1} . Thus it can hardly be resolved in PL.

As we observe only one NP line at 2 K the 1.047 eV emission can belong to an internal 3d transition of either a d^1 (ground state 2E), a d^2 (ground state 3A_2), a d^5 (ground state 6A_1), or a d^7 (ground state 4A_2) configuration, which show no splitting of the ground state in the tetrahedral environment of the four nitrogen atoms. A possible weak splitting caused by the hexagonal crystal field (reduction to C_{3v}) is not observed. A reason is the relatively large line width of about 1.5 meV at 2 K.

We can exclude the d^1 configuration because this configuration has no excited state. The appearance of the excited state in the PL excitation spectrum (Fig. 3) cannot be explained with a d^1 configuration. $\text{Fe}^{3+}(3d^5)$ can be excluded because the 1.3 eV emission is already identified as Fe^{3+} . The linewidth of 1.5 meV for the 1.047 eV NP line is rather large for Zeeman studies. Preliminary Zeeman measurements up to 7 Tesla show no shift of the maximum of the 1.047 eV NP line. With increasing magnetic field the linewidth gets broader but the lineshape of the NP line remains symmetric. Thus we can also exclude the ${}^4T_1 \rightarrow {}^6A_1$ spin-flip transition of $\text{Mn}^{2+}(3d^5)$. For Mn^{2+} we expect a fine structure splitting and Zeeman behavior caused by a Jahn-Teller distortion similar to Fe^{3+} ,¹³ which is not observed here. The decay time of less than a few μs supports the exclusion of the ${}^4T_1 \rightarrow {}^6A_1$ spin-flip transition of a d^5 configuration, which has typical decay times in the ms range.

The following 3d elements have a d^2 or d^7 electronic configuration that can fit to the experimental results on the 1.047 eV emission: $\text{Sc}^+(d^2)$, $\text{Ti}^{2+}(d^2)$, $\text{V}^{3+}(d^2)$, $\text{Cr}^{4+}(d^2)$, $\text{Fe}^+(d^7)$, $\text{Co}^{2+}(d^7)$, and $\text{Ni}^{3+}(d^7)$.

Sc^+ (scandium is a very rare element) and Cr^{4+} (our samples are n-type samples and the element is in its luminescence charge state already in the dark) can be most definitely excluded. The two remaining possible contaminants with d^2 configuration are Ti^{2+} and V^{3+} . For V^{3+} we expect a splitting of the excited state in the range of 1–2 meV instead of 8 meV as observed here. In general the excited state splitting of 8 meV of the 1.047 eV emission is too large for the ${}^3T_2(\text{F})$ state. Also the shape of the excitation band at about 1.6 eV is completely atypical for the ${}^3A_2(\text{F}) \rightarrow {}^3T_1(\text{F})$ transition of Ti^{2+} and V^{3+} (See for example Fig. 6 in Ref. 14 and Fig. 2 and Fig. 3 in Ref. 19). Baur *et al.* already identify a NP line at 0.94 eV, which shows an excited state at 1.5

meV above the ground state, with V^{3+} .¹⁸ Our studies on the 1.19 eV emission indicate that this emission is caused by the Ti^{2+} center.¹⁴ For the reasons mentioned above a transition metal with a $3d^2$ electronic configuration can be excluded to cause the 1.047 eV emission. According to the experimental observations only a $3d^7$ electronic configuration can explain the 1.047 eV emission.

Fe^+ (1.3 eV emission is due to Fe^{3+}) can most definitely be excluded. A possible attribution is nickel in its $3+$ charge state. But from PLE we know that the luminescence center is already present in the samples without illumination. We expect Ni^+ and Ni^{2+} to be the stable configurations in the dark in n-type GaN material. We cannot completely exclude the ${}^4T_2(F) \rightarrow {}^4A_2(F)$ transition of Ni^{3+} , but it is improbable in n-type GaN.

We know that cobalt is not a dominant natural contamination in crystal growth, but it is the best candidate that explains the present experimental results on the 1.047 eV emission in the n-type samples. The attribution to a 3d element in the $2+$ charge state (e.g., Co^{2+}) is in accordance with the observation of PL excitation spectroscopy that the 3d element is in its luminescent charge state in the dark in the n-type samples. The 1.047 eV emission can be attributed to the ${}^4T_2(F) \rightarrow {}^4A_2(F)$ transition of Co^{2+} . The observed splitting of 8 meV (see inset of Fig. 1) for the ${}^4T_2(F)$ state caused by spin-orbit coupling is reasonable. The absorptions at about 1.6 eV observed in PL excitation spectroscopy can be attributed to the ${}^4A_2(F) \rightarrow {}^4T_1(F)$ transition of Co^{2+} .

Taking into account the suggested conduction band offset of 0.9 eV between GaN and GaAs²⁰ the assignment to Co^{2+} explains why the excited states appear in the bandgap. In GaAs the Co^{2+} ground state is located about 0.14 eV above the valence band.²¹ Therefore, according to the rule of Langer and Heinrich²² the Co^{2+} ground state is located in GaN about 2.2 eV below the conduction band. This explains the appearance of the 1.6 eV excited state in the bandgap of GaN as observed in the excitation spectrum of the 1.047 eV emission.

However, it has to be emphasized that the rule of Langer and Heinrich²² must be used with care. Baur *et al.*⁶ predict a conduction band offset between GaN and AlN of 2.3 eV from their Fe^{2+} ground state levels applying the Langer and Heinrich rule. If we use this result and the position of the Fe^{2+} ground state in GaAs (0.49 eV above the valence band²¹) we can deduce the band offset between GaAs and GaN. We find that the conduction bands of GaAs and GaN are nearly resonant. But this result contradicts the effective conduction band offset of 0.9 eV between GaAs and GaN obtained by G. Martin *et al.*²⁰

V. CONCLUSION

In a nutshell, we performed near infrared photoluminescence spectroscopy on GaN grown by the sandwich technique. We found three emissions due to internal electronic transitions of 3d elements, which appear as natural contaminants in the GaN layers. Besides the luminescence bands

with no-phonon lines at 1.3 eV (Fe^{3+} , ${}^4T_1 \rightarrow {}^6A_1$) and 1.19 eV (Ti^{2+} , ${}^1E(D) \rightarrow {}^3A_2(F)$), which both were also detected in GaN samples grown on sapphire by MOVPE and VPE, we observe an additional strong no-phonon line at 1.047 eV with a GaN related phonon sideband. The excited state of the 1.047 eV emission shows a fine-structure splitting of 8 meV. The appearance of a further excited multiplet state at about 1.6 eV in photoluminescence excitation measurements shows that the defect is already in its luminescent charge state in the dark in n-type GaN. The 1.047 eV emission is attributed to a 3d element with an electronic d^7 configuration. From the present results Co in its $2+$ charge state is the most probable natural contender to cause the 1.047 eV luminescence band in the n-type material.

ACKNOWLEDGMENTS

The authors are indebted to Y. A. Vodakov, A. D. Roenkov, and S. Fischer for the supply of samples. The financial support of the Deutsche Forschungsgemeinschaft (DFG) is gratefully acknowledged.

- ¹H. Amano, M. Kito, K. Hiramatsu, and I. Akasaki, *Jpn. J. Appl. Phys.* **28**, L2112 (1989).
- ²S. Nakamura, T. Mukai, and M. Senoh, *J. Appl. Phys.* **76**, 8189 (1994).
- ³A comparison on the three wide gap semiconductors SiC, GaN, and ZnSe is given by: H. Morkoç, S. Strite, G.B. Gao, M.E. Lin, B. Sverdlov, and M. Burns, *J. Appl. Phys.* **76**, 1363 (1994).
- ⁴K. Maier, M. Kunzer, U. Kaufmann, J. Schneider, B. Monemar, I. Akasaki, and H. Amano, Proc. of the 17th International Conference on Defects in Semiconductors, Gmunden, Austria [*Material Sci. Forum* **143-147**, 93 (1994)].
- ⁵J. Baur, K. Maier, M. Kunzer, U. Kaufmann, J. Schneider, H. Amano, I. Akasaki, T. Detchprohm, and K. Hiramatsu, *Appl. Phys. Lett.* **64**, 857 (1994).
- ⁶J. Baur, K. Maier, M. Kunzer, U. Kaufmann, and J. Schneider, *Appl. Phys. Lett.* **65**, 2211 (1994).
- ⁷P.S. Whitney, K. Uwai, H. Nakagome, and K. Takahei, *Electron. Lett.* **24**, 741 (1988).
- ⁸W. Körber, J. Weber, A. Hangleiter, K.W. Benz, H. Ennen, and H.D. Müller, *Appl. Phys. Lett.* **79**, 741 (1986).
- ⁹Y.A. Vodakov, E.N. Mokhov, A.D. Roenkov, and D.T. Saidbekov, *Phys. Status Solidi A* **51**, 209 (1979).
- ¹⁰Y.A. Vodakov, M.I. Karklina, E.N. Mokhov, and A.D. Roenkov, *Inorganic Mater.* **17**, 537 (1980).
- ¹¹C. Wetzel, D. Volm, B. K. Meyer, K. Pressel, S. Nilsson, E. N. Mokhov, and P. G. Baranov, *Mater. Res. Soc. Symp. Proc.* **393**, 453 (1994).
- ¹²C. Wetzel, D. Volm, B. K. Meyer, K. Pressel, S. Nilsson, E.N. Mokhov, and P. G. Baranov, *Appl. Phys. Lett.* **65**, 1033 (1994).
- ¹³R. Heitz, P. Thurian, I. Loa, L. Eckey, A. Hoffmann, I. Broser, K. Pressel, B.K. Meyer, and E.N. Mokhov, *Appl. Phys. Lett.* **67**, 2822 (1995).
- ¹⁴R. Heitz, P. Thurian, I. Loa, L. Eckey, A. Hoffmann, I. Broser, K. Pressel, B. K. Meyer, and E. N. Mokhov, *Phys. Rev. B* **52**, 16 508 (1995).
- ¹⁵T. Kozawa, T. Kachi, H. Kano, Y. Taga, M. Hashimoto, N. Koide, and K. Manabe, *J. Appl. Phys.* **75**, 1098 (1994).
- ¹⁶Landolt-Börnstein, *Numerical Data and Functional Relationships in Science and Technology* (Springer, Berlin, London, 1982), New Series III/17b, p. 46.
- ¹⁷R. Heitz, A. Hoffmann, and I. Broser, *Phys. Rev. B* **45**, 8977 (1992).
- ¹⁸J. Baur, U. Kaufmann, M. Kunzer, J. Schneider, H. Amano, I. Akasaki, T. Detchprohm, and K. Hiramatsu, *Appl. Phys. Lett.* **67**, 1140 (1995).
- ¹⁹B. Clerjaud, C. Naud, B. Deveaud, B. Lambert, B. Plot, G. Bremond, C. Benjeddou, G. Guillot, and A. Nouailhat, *J. Appl. Phys.* **58**, 4207 (1985).
- ²⁰G. Martin, S. Strite, J. Thornton, and H. Morkoç, *Appl. Phys. Lett.* **58**, 2375 (1991).
- ²¹B. Clerjaud, *J. Phys. C: Solid State Phys.* **18**, 3615 (1985).
- ²²J.M. Langer and H. Heinrich, *Phys. Rev. Lett.* **55**, 1414 (1985).